Parameterising a generic model for the dynamic energy budget of Antarctic krill, *Euphausia superba*

Tjalling Jager[1,*], Elisa Ravagnan[2]

[1] Dept. of Theoretical Biology, VU University Amsterdam, de Boelelaan 1085, NL-1081 HV, Amsterdam, the Netherlands. Email: tjalling.jager@vu.nl
[2] IRIS Environment, International Research Institute of Stavanger, Mekjarvik 12, 4070 Randaberg, Norway.

ABSTRACT: Dynamic Energy Budget (DEB) theory is a generic and comprehensive framework for understanding bioenergetics over the entire life cycle of an organism. Here, we apply a simplified model derived from this theory (DEBkiss) to Antarctic krill (*Euphausia superba*). The model is parameterised using growth curves, and conversion factors for body composition and length-weight relationships. Subsequently, the model is used to predict a series of life-history traits (as function of body size) that were not used for parameterisation: instantaneous growth rates, ingestion and respiration rates, weight loss on starvation, and the number of eggs produced at spawning. Within the DEB framework, these traits are not intrinsic properties of the organism, but tightly-coupled model outputs that depend on body size, life stage, and environmental conditions. Overall, the model predictions are consistent with the patterns in the (rather uncertain) observations, lending credence to the model assumptions underlying the DEBkiss model. More work is needed to fully elucidate the bioenergetics of the *E. superba* life cycle, but this analysis demonstrates how a dynamic budgeting framework can ensure consistency among the different life-history traits. Thereby, such models help in the interpretation of experimental results and the comparison of species, but can also form the basis for predicting population dynamics and the impacts of stressors.

KEY WORDS: Antarctic krill . *Euphausia superba* . Dynamic Energy Budget . life history traits . DEBkiss

INTRODUCTION

Krill are an important component of marine food webs, both ecologically and economically. Therefore, quantitative knowledge about krill life histories is essential for predicting the impact of anthropogenic disturbances, such as commercial fishing (Nicol et al. 2012) and pollution (Bengtson Nash et al. 2008), on their populations. To understand the life history in a quantitative manner, considering the energy budget is extremely helpful as all organisms have to obey the conservation laws for mass and energy. The most comprehensive and best-tested approach in the field of biological energetics is Dynamic Energy Budget (DEB) theory (Nisbet et al. 2000, Kooijman 2001). This theory embodies a consistent and species-independent formalisation of the rules for metabolic organisation. DEB theory aims to explain feeding, growth, development and reproduction of individuals throughout their complete life cycle (from egg to death) in a single framework, as a function of the environmental conditions (food availability, temperature, toxicants, etc.). Models based on DEB theory have already been extensively applied in marine ecophysiology for a range of species (see Alunno-Bruscia et al. 2011), and can lay the foundation for population models (see Jager et al. 2014).

The simplest complete DEB model is the 'standard animal' model (Sousa et al. 2010). However, this model is already rather complex, and its parameterisation challenging (Lika et al. 2011). Recently, a more simplified energy-budget approach was presented in the form of DEBkiss (Jager et al. 2013), which follows the general structure of DEB theory with a few shortcuts. These simplifications allow for a more direct and intuitive link to experimental data, while maintaining the explicit mass conservation over the life cycle. Here, we parameterise DEBkiss for the Antarctic krill, *Euphausia superba*, a key species in the Antarctic food web for which a large body of literature has been established. It is important to realise that the model parameters are abstract quantities that cannot be directly measured. However, the complete parameter set governs all life-history traits over the entire life cycle, and hence, a more indirect parameterisation is feasible. Here, we demonstrate how model parameters can be derived from literature data on growth and composition only, and how these parameters can be used to predict model outputs (instantaneous growth, ingestion, respiration, starvation and reproduction) as a function of body size.

It must be stressed that we focus here on obtaining the parameters of the energy budget, and not on producing an accurate description of the life cycle of *E. superba* under actual field conditions. In principle, the parameters of the energy budget remain constant with ontogeny, although some specific deviating patterns have been observed (Kooijman Acc.). Furthermore, the model parameters vary in a predictable manner with changes in the environment; specifically with temperature and food availability (Saraiva et al. 2012). Therefore, a parameterised energy-budget model can be expected to produce a realistic life history under field conditions, provided that the environmental forcings are realistically quantified. Or it can be used vice versa to reconstruct environmental forcings based on observed patterns in growth and/or reproduction, or even from examining calcified structures like otoliths in fish (Pecquerie et al. 2012). And finally, DEB-based models can be applied to explain and to predict the effects of stressors (such as toxicants) on all traits over time (Jager et al. 2014). All these applications, however, depart from a parameterised model for the species, and here we present a first attempt to produce and test such a model for *E. superba* using data from the literature.

METHODS

The DEBkiss model

DEBkiss (Jager et al. 2013) is a simplified model for animals, derived from DEB theory, and schematically shown in Figure 1. The main difference with the standard DEB animal model (Sousa et al. 2010) is the absence of a reserve compartment in between assimilation and the energy-requiring metabolic processes; the assimilates obtained from feeding are used directly to fuel growth, development, maintenance and reproduction. Storage of assimilates is treated in the form of a 'reproduction buffer', and hence located in the $1\text{-}\kappa$ branch of the scheme in Figure 1. We assume that this buffer is used to fuel spawning events, and can also be used to pay maintenance costs when the assimilation flux is insufficient to cover these expenses (Jager et al. 2013). The embryo assimilates a buffer of storage material that is provided by the mother in the egg, but otherwise follows the same rules as the feeding juvenile stages. Birth, in a DEB context, marks the start of external feeding, which may thus be preceded by hatching (as is the case in krill). The buffer of assimilates provided in the egg thus has to sustain the developing animal until it reaches the first feeding stage.
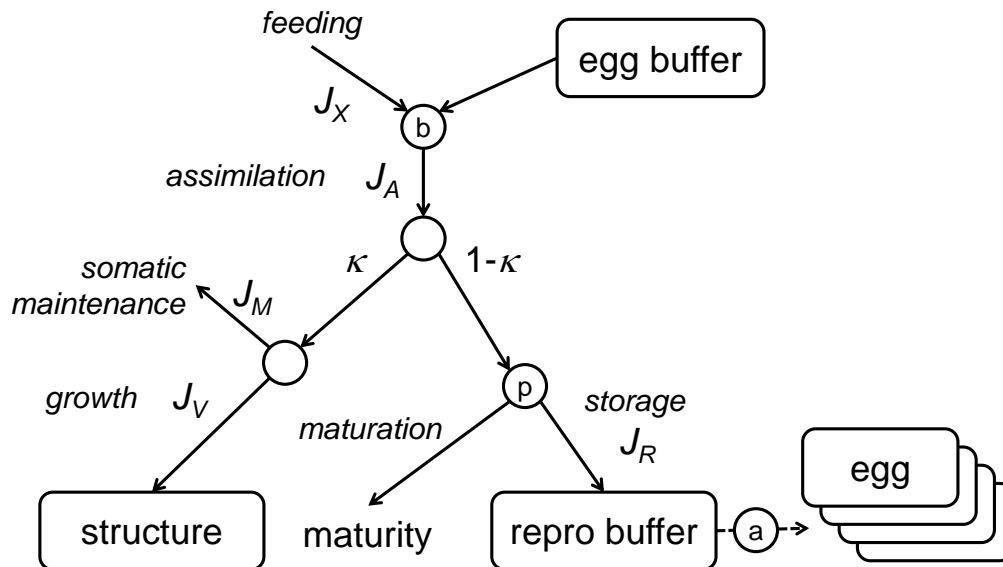

Figure 1. Schematic representation of the mass flows in a DEBkiss model. At 'birth', assimilation switches from the egg buffer to external food (the node 'b'). The assimilation flux is continuously split into a constant fraction κ to the soma (for structure and somatic maintenance), and $1\text{-}\kappa$ to maturation, which is switched to the reproduction buffer at 'puberty' (the node 'p'), and transformed into eggs in adults (the node 'a').

Table 1. Model equations for the basic model as depicted in Figure 1. Model parameters are explained and in Table 2. For the state variables, $t = 0$ marks the start of embryonic development.

Fluxes	Specification (mg$_{dwt}$/d)
Assimilation	$J_A = f J_{Am}^a L^2$
Somatic maintenance	$J_M = J_M^v L^3$
Structural growth	$J_V = y_{VA}(\kappa J_A - J_M)$
Feeding	$J_X = J_A / y_{AX}$
Investment reproduction buffer ($L_w > L_{wp}$)	$J_R = (1 - \kappa) J_A$

State variables	Specification (mg$_{dwt}$)
Structural body mass	$\dfrac{d}{dt} W_V = J_V$ with $W_V(0) \approx 0$
Assimilate buffer in egg	$\dfrac{d}{dt} W_B = -J_A$ with $W_B(0) = W_{B0}$
Build-up of reproduction buffer	$\dfrac{d}{dt} W_R = J_R$ with $W_R(0) = 0$

Conversions	Specification
Volumetric length to dry weight	$W_V = d_V L^3$
Volumetric length to physical length	$L_w = L / \delta_M$

The model is described in detail in Jager et al. (2013). However, the set of equations that is relevant for the current data analysis is provided in Table 1, and all model parameters are explained in Table 2, along with their value and units. An extended summary of the model equations, underlying assumptions, and some derivations, are provided in Supplement 1.

The measures of body size that are used in DEBkiss are the structural dry weight W_V and the volumetric length L. The latter is the cubic root of structural body volume (L^3, volume of the structure compartment, and hence excluding any storage buffers). Volumetric length is related to physical length (L_w, e.g., total body length) by a shape correction coefficient (δ_M, see Table 1). When the animal does not change in shape during growth (isomorphy), δ_M will be constant with ontogeny. Food availability is represented in a simplified manner, introducing the scaled functional response f, such that $f = 1$ is ad libitum food availability (of optimal quality) and $f = 0$ complete starvation. Many of the specific aspects of food availability and feeding behaviour thus boil down to a change in f.

In the scheme of Figure 1, the κ branch of assimilates is used for maintenance and growth, whereas the 1-κ branch is used for maturation and filling of the reproduction buffer. The investment in maturation is assumed to be burnt, and hence does not increase biomass. At some point in the life cycle ('puberty'), the investment to maturation is switched to the reproduction buffer. The logic of this switch can be observed in species that reproduce (almost) continuously, as the start of reproduction does not affect the growth curve (see e.g., Nisbet et al. 2000, Jager et al. 2013). Antarctic krill, however, do not reproduce continuously when mature, but rather produce large batches of eggs in the summer season. Furthermore, like many species exposed to strong seasonality, they build up a storage buffer to survive the winter period of low food availability (Hagen et al. 2001). Here, we suggest addressing both features with a single buffer in the 1-κ branch. The position in this branch of the allocation scheme ensures that the start of

4

storage build-up does not influence structural growth, and that the build-up can continue in fully-grown adults (both of which seem realistic).

In DEB theory, puberty marks the cessation of maturation, and the complete investment into the 1- κ branch is switched to the reproduction buffer. Here, we tentatively stick to that assumption, but it may be more realistic to assume that maturation and storage occur simultaneously (or alternatingly, e.g., depending on the season) in juveniles, and possibly even in adults, as stored lipids can be used for gonad maturation (Teschke et al. 2008). We position the start of investment into storage ('puberty') at the moult from furcilia VI to juvenile, as furcilia larvae do not seem to build up much of a storage for the winter, in contrast to juveniles (Hagen et al. 2001, Meyer 2012). These allocation rules for the 1-κ branch should be treated as provisional as data on the build-up of storage under known feeding conditions are lacking (a preliminary analysis using lipid data from field-sampled animals is presented in Supplement 2).

Deviations from the standard allocation rules are needed under starvation conditions, when the investment into the soma is insufficient to cover the costs of maintenance ($\kappa J_A < J_M$). In the standard DEBkiss model, growth stops on starvation, and maintenance is paid from the 1-κ branch (which also implies that the reproduction buffer is drawn upon). As there are no reports of structural growth continuing on starvation, this assumption seems to hold for *E. superba* as well. If the 1-κ branch cannot yield sufficient resources to fuel maintenance, structure will be burnt and the individual will shrink. Krill can survive considerable shrinkage in structure, although starvation also leads to a reduction in respiration rates (Ikeda & Dixon 1982), presumably due to a reduction in maintenance costs.

All rate constants (the model parameters in Table 2 that have time in their dimension) are affected by temperature. We can expect that all rate constants change with temperature by the same factor, and the Arrhenius relationship is generally applied in this context (see Supplement 1).

Model predictions

The parameterised model can subsequently be used to make independent predictions for other life-history traits. A number of studies report instantaneous growth rates (on length basis) from field-sampled animals. The model prediction for this trait follows from the growth flux on mass basis (derivation in Supplement 1):

$$\frac{d}{dt} L_W = \frac{J_V}{3 d_V L^2 \delta_M} \qquad [1]$$

This growth rate (in mm/d) depends on the food availability as J_V depends on J_A, which in turn depends on f (see Table 1).

Ingestion and respiration rates are often expressed in the literature on carbon basis to facilitate their quantitative comparison. Here, we consistently express both ingestion and respiration rates as daily carbon ration (ingested or respired carbon weight per carbon body weight per day). In DEBkiss, the specific ingestion rate is a model output, and it is not constant but decreases with body size (as feeding scales with a surface area and carbon weight with a volume):

$$J_X^c = \frac{J_A}{y_{AX}^c L^3 d_V} \qquad [2]$$

Note that neither the carbon content of the organism nor that of the food appears in this equation, as we assume that assimilates have the same composition as biomass, and we take the assimilation efficiency y_{AX}^c on carbon basis. The predicted daily ration also depends on the food availability, as J_A depends on the scaled functional response f (see Table 1).

In a DEB context, respiration constitutes all the dissipation processes in which assimilates are burnt to do work (in aerobic respiration, this relates to the use of oxygen and the production of carbon dioxide). An important aspect of respiration is of course maintenance, but also included are the overheads of transformation processes (in feeding, in growth, and in production of eggs). Furthermore, assimilates allocated to the maturation process do not contribute to biomass but are burnt to increase the maturity status. The maximum possible respiration flux (J_{D+} in mg_{dwt}/d) is given by the assimilation flux minus the flux fixed in biomass. In juveniles, only structural growth is fixed in biomass (the maturation flux is assumed to be burnt), whereas in adults, also the flux allocated to the reproduction buffer is not dissipated:

$$J_{D+} = J_A - J_V \qquad \text{(when } L_w < L_{wp}\text{)}$$
$$J_{D+} = J_A - J_V - J_R \quad \text{(when } L_w \geq L_{wp}\text{)}$$

[3]

It should be noted that we assume here that the switch from maturation to storage is complete and immediate, at a fixed body length L_{wp}.

In a starving individual, growth will cease, and it is likely that maturation can be decreased as well. The minimum respiration thus constitutes the somatic maintenance flux ($J_{D-} = J_M$). However, animals overwintering (Meyer 2012) or under prolonged starvation (Ikeda & Dixon 1982) may be able to reduce these maintenance costs, which would result in lower respiration rates than predicted. It should be noted that we ignored losses in the feeding process, which is acceptable for our purpose as animals are usually not fed during respiration measurements. Measured respiration rates should lie within the two extremes outlined above. Where they end up depends on the experimental duration (the degree of starvation) and the life stage. We can easily convert model predictions for J_D to a specific flux on carbon basis as follows:

$$J_D^c = \frac{J_D}{d_V L^3}$$

[4]

Note that the carbon content of the organism does not appear in this equation, as we assume that assimilates that are burnt have the same composition as biomass. In this calculation, the maximum respiration on carbon basis will decrease with size, as growth will decrease, and assimilation per unit of weight as well (as assimilation scales with body surface area). The minimum respiration on carbon basis is independent of size as the somatic maintenance flux scales with body volume. Several life stages include a storage: the egg buffer for the embryo and non-feeding larvae, and the seasonal overwintering/reproduction buffer in juveniles/adults. The predictions for carbon-specific ingestion and respiration rates are based on structural weight only. If measurements are made on individuals with a considerable storage, we can expect lower rates than predicted.

Weight loss on complete starvation is assumed here to result from the use of structural biomass to pay the somatic maintenance costs. We assume that other energy-requiring processes (growth, maturation, reproduction) are completely stopped. This results in an exponential decay of the body volume, with as rate constant (Jager et al. 2013):

$$k_S = \frac{J_M^v}{y_{AV}d_V} \tag{5}$$

The yield factor y_{AV} is less than one, as mass is lost in the transformation of structure to pay somatic maintenance costs.

For a simple estimation of the reproductive output, we can assume that the female does not grow substantially during the build-up of the reproduction buffer, that the total mass flux into the 1-κ branch is used for egg production, and that the animal is feeding at the maximum rate ($f = 1$). The clutch size (ΔR) then depends on the available time to build up the buffer (Δt):

$$\Delta R = \frac{y_{BA}(1-\kappa)J_A}{W_{B0}}\Delta t \tag{6}$$

Treatment of literature data

Data were extracted from graphs in the original publications using the freeware PlotReader (http://jornbr.home.xs4all.nl/plotreader). All model calculations were performed in Matlab. Model optimisations were performed on the growth curves by maximising the likelihood function, assuming a normal distribution of the residuals after square-root transformation (Jager & Zimmer 2012). No attempts were made to correct the data to reflect different experimental temperatures as other uncertainties will likely dominate anyway (most experiments were done between -1 and 1 °C).

Data on the instantaneous growth rate were taken from Kawaguchi et al. (2006), Atkinson et al. (2006), Daly (2004), Meyer et al. (2009), Quetin et al. (2003), and Ross et al. (2000). All these data were obtained from field-collected animals. Spring and summer values were used for juveniles and adults, and autumn or late winter values for furcilia.

Experimental data on ingestion rates were taken from the publications of Kato et al. (1982), Meyer et al. (2002), Meyer et al. (2003), Meyer & Oettl (2005), Pakhomov et al. (1997), Pakhomov et al. (2004), Ikeda (1984), Haberman et al. (2003), Boyd et al. (1984), Schnack (1985), Clarke et al. (1988), Daly (1990), Daly (1998). Respiration rates were taken from the publications of Kato et al. (1982), Hirche (1983), Meyer et al. (2002), Meyer et al. (2010), Meyer et al. (2003), Meyer et al. (2003), Ikeda (1981), Ikeda & Mitchell (1982), Torres et al. (1994), Daly (1998), Ishii et al. (1987), Segawa et al. (1982). All ingestion and respiration rates were expressed as carbon-specific values in mg$_C$ ingested or respired per mg$_C$ body weight per day. If a conversion was needed, we used the food carbon content provided by the original authors or the conversion factors from Table 2. If multiple food levels were used for ingestion rates, only the results from the highest levels were included here. For respiration, we did not use winter values for the comparisons, which are roughly a factor of 2 (Torres et al. 1994) to 4 (Meyer et al. 2010) lower in juvenile/adult Antarctic krill than in summer. Furthermore, we only used data for the feeding stages (calyptopis and later) to avoid complications of the remaining egg buffer.

Experimental data on clutch sizes at known body lengths were taken from Denys & McWhinnie (1982), Harrington & Ikeda (1986), Nicol et al. (1995), and Ross & Quetin (1983).

MODEL PARAMETERISATION

Deriving fixed model parameters

The yield factors y_{VA} and y_{AV} are difficult to establish from experimental data, and hence defaults (Jager et al. 2013) are provided in Table 2. The yield of assimilates on food (y_{AX}), or assimilation efficiency, can be expressed in various ways. If we take y_{AX} on dry-weight basis, its value will strongly depend on the composition of the food. As most measured ingestion rates are reported on carbon basis, we will take y_{AX} on carbon basis too, for which 80% seems to be a reasonable value (Kato et al. 1982, Meyer et al. 2003). The allocation fraction to the soma (κ) can be determined from experimental data, but generally requires a combination of detailed growth and reproduction observations over time (at constant environmental conditions). As such data are not available for *E. superba*, we will depart from the typical value (Lika et al. 2011) for this fraction in Table 2. The egg dry weight is taken from Ikeda (1981), and the approximate sizes for the start of the juvenile (L_{wp}) and adult (L_{wa}) stages from Ikeda (1985a).

Conversions for body size and composition

Based on very similar figures mentioned for furcilia VI (Ikeda 1984) and *E. superba* in general (Ikeda & Mitchell 1982), we select a dry-weight density $d_V = 0.22$ mg/mm^3 for all stages. The shape correction coefficient (δ_M) can be determined from measurements of length and fresh weight on the same individuals. Using the data of Hofmann & Lascara (2000) for larger individuals (10-60 mm), as well as the data from Nicol et al. (1995) for spent females, we obtain a rather constant value $\delta_M = 0.20$. For larvae cultivated under laboratory conditions (Ikeda 1984), the shape correction coefficient is large for the early nauplii, and then rapidly drops to a stable level of around $\delta_M = 0.20$ in the calyptopis I stage. Apparently, early growth is not isomorphic. As this deviation is only relevant for the non-feeding nauplius and metanauplius stages (for which we did not need to make any conversions), we will not go into further detail here. For the carbon content of *E. superba* we selected a typical value of 0.45 mg$_C$/mg$_{dwt}$ based on the values provided in several publications (Ikeda & Mitchell 1982, Hirche 1983, Ikeda 1984). For respiration data, we often need to convert volume of oxygen used to weight of carbon converted to CO_2. Using the density of oxygen, the atomic weights of oxygen and carbon, and assuming a respiration quotient of 0.9, we arrive at a conversion factor of 0.48 mg$_C$/ml$_{O2}$ (see Supplement 1).

Table 2. Model parameters and conversion factors with their values.

Symb.	Description	Value	Unit
	Conversion factors		
d_V	dry-weight density	0.22	mg_{dwt}/mm^3
	wet-weight density	1	mg_{wwt}/mm^3
δ_M	shape-correction coefficient (for $L_w > 2$ mm)	0.20	[-]
	carbon weight per dry weight	0.45	mg_C/mg_{dwt}
	carbon weight per oxygen volume in respiration	0.48	mg_C/ml_{O2}
	Fixed model parameters		
y_{AX}^c	yield of assimilates on food (carbon based)	0.8	mg_C/mg_C
y_{VA}	yield of structure on assimilates	0.8	mg_{dwt}/mg_{dwt}
y_{AV}	yield of assimilates on structure (starvation)	0.8	mg_{dwt}/mg_{dwt}
y_{BA}	yield of storage buffer on assimilates	0.95	mg_{dwt}/mg_{dwt}
κ	fraction allocation to soma	0.8	[-]
W_{B0}	dry weight of a single egg	0.028	mg_{dwt}
L_{wp}	physical length at start of juvenile stage	11	mm
L_{wa}	physical length at start adult stage	35	mm
	Model parameters from growth curves (0 °C)		
J_{Am}^a	maximum area-specific assimilation rate	0.044	$mg_{dwt}/mm^2/d$
J_M^v	volume-specific somatic maintenance rate	0.0032	$mg_{dwt}/mm^3/d$
f_B	apparent f for assimilation of egg buffer	0.28	[-]
f	scaled functional response		[-]
	juvenile/adult, data Ikeda (1985a)	1	
	juvenile/adult, data Ikeda (1987)	0.85	
	furcilia, data Ikeda (1984)	0.34	

Analysing growth curves

Growth curves contain information on specific assimilation (J_{Am}^a) and specific maintenance (J_M^v) rates. The specific maintenance governs the curvature of the growth curve, and hence the time to reach 95% of the asymptotic size. Specific assimilation determines the initial growth rate (in mm/d) and, together with the specific maintenance, the maximum size. Laboratory growth curves are most useful for this purpose as the environmental conditions can be kept constant over the duration of the experiment.

Ikeda (1987) presents growth data for two individuals (one male and one female) over 3 years in the laboratory at 0 °C. Size measurements started after the moult from furcilia VI to juvenile, so this point is taken as $t = 0$ here. A second data set was derived from Ikeda (1985a), who compiled several data sets to provide a theoretical maximum growth curve over the entire life cycle, for which we assume $f = 1$. For the juvenile/adult stages (larval stages will be dealt with separately), we extracted a large number of points from this curve, which are thus not actual size measurements. The first thing to note is that the three growth curves do not overlap. The individual male and female are assumed to differ in initial size only, which suffices to capture the differences in their growth patterns. However, their growth is slower than the maximum

curve, and their asymptotic size is also less than that of the maximum growth curve, and less than the maximum size of the species, which is around 60 mm physical length (Ikeda 1985a), or 12 mm volumetric length. We suggest that this difference is caused by a difference in the quantity or quality of the food, and hence allow for a lower value of *f* for the data of Ikeda (1987), keeping all other parameters the same.

The growth curve corresponds to the expected von Bertalanffy pattern (Figure 2), but around the maximum asymptotic size, the data for the two individuals become more variable. The reasons for this are unclear. The fitted model parameters for assimilation and maintenance are given in Table 2 (no confidence intervals are provided as the points in the maximum growth curve do not represent measurements). These parameters yield an asymptotic size of 55 mm, which is still a bit too small. It is possible that the maximum growth curve of Ikeda (1985a) still does not represent the optimal conditions for the species (and may thus represents *f* < 1).
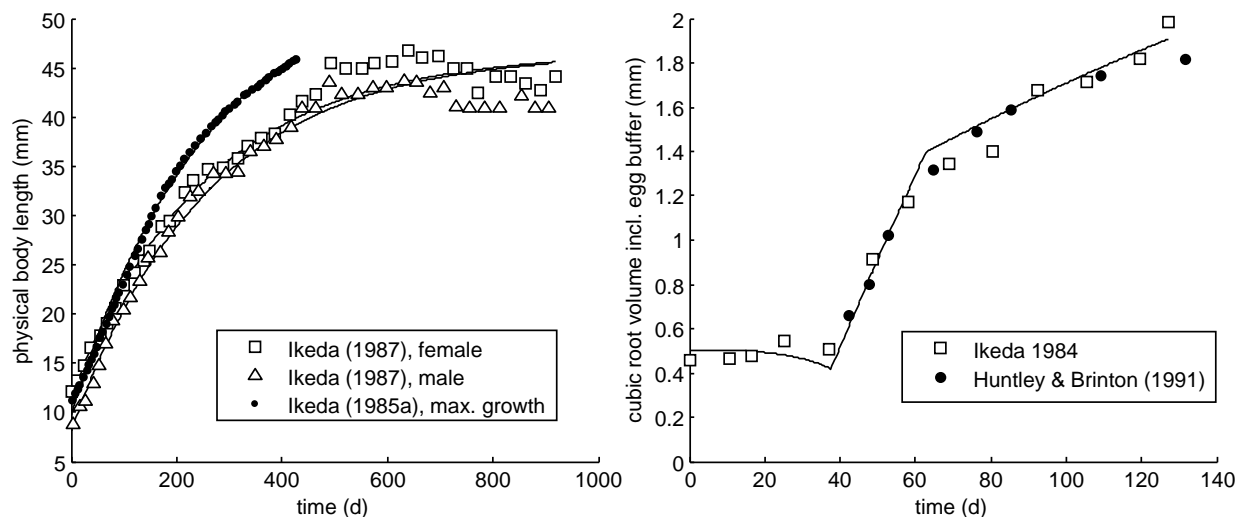

Figure 2. Fit to size data for juvenile/adults (left panel), and egg/larvae (right panel). The left panel shows data for two individuals (Ikeda 1987), and the maximum growth curve suggested by Ikeda (1985a). The model fit (solid lines) assumes the same parameters for all data sets, but a lower food availability for the two individuals (Table 2). The right panel shows data for larvae. The model fit (solid line) is to data of Ikeda (1984) and assumes the same parameters as for the juveniles/adults but a different food availability for both the non-feeding and furcilia larval stages (Table 2). The start of external feeding is forced to 37 days, and the moult to furcilia I at 63 days. Data of Huntley & Brinton (1991) are shown for comparison, with their time axis shifted to match the growth pattern of the model.

Ikeda (1984) presents data for growth of larvae (egg to furcilia VI). At the end of the experiment, the animals are still far away from their asymptotic size, and hence there is no possibility to estimate the specific maintenance rate, which was fixed to the value from the previous fit on juveniles/adults. The reported developmental time for each stage (and thus each size determination) is at the start of the stage. For fitting and plotting, we modified the time vector to represent the more representative developmental time half-way into the stage. Calyptopis I is the first feeding stage for Antarctic krill, and the data of Ross & Quetin (1989) show that the yolk from the egg is used up to half-way into this stage. Therefore, we constrain the fit so that 'birth' (start of external feeding) is positioned at *t* = 37 d post egg deposition (including into the likelihood function the probability density for the predicted hatching time in a normal distribution with mean of 37 days and s.d. of 1 day).

Using the specific assimilation for the juvenile/adult stages leads to two misfits on this data set. Firstly, it underpredicts the observed time for the start of external feeding ('birth'), and it overpredicts the observed growth rate for the furcilia stages. The mismatch for the age at birth seems to be a common situation when using DEB models for several taxonomic groups, especially those sporting larval stages (Kooijman Acc.). For now, we correct this deviation by assuming a lower apparent food availability for the non-feeding stages (f_B). The model predicts a decrease in total volume for the non-feeding stages (due to dissipation of the egg buffer), whereas the data actually suggest a small increase. This discrepancy is probably caused by an increase in the water content of the first larval stages (Ikeda 1985b).

For the feeding larval stages, the growth rate of the calyptopis stages is well captured by the model. The growth rate of the furcilia stages is however considerably smaller than predicted. Here, we fit an independent (lower) value of f for the furcilia, which yields a good correspondence to the data. It is unclear why the feeding rate should be lower for this stage. One possibility is some form of food limitation of the larvae, perhaps caused by less efficient feeding of these stages and/or improper food selection in the experiment. The reconstructed growth curve for field-collected animals of Huntley & Brinton (1991) closely matches the laboratory data of Ikeda when expressed on volumetric length (Figure 2), which indicates that this behaviour is not an experimental artefact. As an alternative explanation, a temporary switch in parameter values might occur in this stage, e.g., a lower value for J_{Am}^a or κ (see Kooijman Acc.), but this cannot be further investigated without more detailed experimental work.

Comparing the data set for larvae (Ikeda 1984) with the two individuals (Ikeda 1987), a timing mismatch becomes apparent. For the individuals, observations started after some 195 days post hatching at a physical length of approximately 10 mm. In the larval experiment, the animals reached a size of 10 mm after some 120 days already. The reason for this discrepancy cannot be elucidated without a more complete data set, but it stresses the dependence of the growth pattern on the specific conditions of the test.

MODEL PREDICTIONS

The model parameters of Table 2 will be used to predict growth rates, ingestion, respiration, starvation and reproduction as a function of body size. All of these life-history traits are model outputs; they result from the model parameters (Table 2), the structure of the model (Figure 1), and the food level that the organisms experience (f). We compare the model predictions to data collected from the literature. Each of these data sets has limitations regarding the methods used, the animals used (usually sampled from the field), and the conditions of the experiment. Therefore, these comparisons should not be seen as a strict validation of our model and its parameterisation, but rather as a means to provide a rough idea of its representativeness. Predictions based on an alternative parameterisation with a low value of κ are provided as Supplement 3.
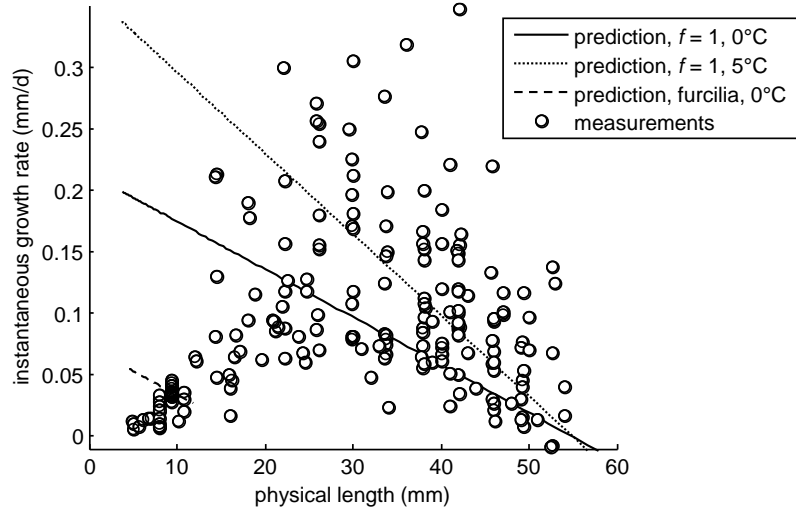
Instantaneous growth rates

Figure 3. Measured and predicted values for the instantaneous growth rate of krill. Model predictions (using Eq. 1) are shown for ad libitum food availability ($f = 1$) at two temperatures (extrapolation to 5°C, see Supplement 1), and for furcilia with a lower functional response (Table 2).

Instantaneous growth rates are generally estimated by measuring the change in (uropod) length with moulting from field-collected animals, in combination with an estimate of the inter-moult period (see e.g., Kawaguchi et al. 2006). As such, they are considered to be representative for the growth rate under field conditions. There is a large variation in the data (Figure 3), which relates to uncertainties in the method (e.g., the estimation of inter-moult period), but also to the unknown environmental factors (food availability and temperature) that the animals experienced in their recent past. Figure 3 shows an additional model prediction for 5°C to show the influence of temperature on the growth rate. Our model prediction is on the lower end of the reported growth rates, which could mean that most data points represent growth rates from animals experiencing field temperatures higher than 0°C. However, we should also consider that our parameterisation based on laboratory data is underpredicting maximum growth rates in the field. Increasing growth rates without increasing maximum length would require increasing the specific assimilation and specific maintenance rates by the same factor (similar to the effect of temperature in Figure 3), with automatic consequences for the other predicted traits. The low growth rates observed for furcilia larvae in Figure 3 are consistent with the laboratory growth curve in Figure 2 (where fitting this stage required a lower value of f, see Table 2).

Ingestion rates

A range of different methods has been used to derive ingestion rates, but in Figure 4, we simply combined the reported values from a number of studies (see Methods section) in a single plot. The DEBkiss prediction for the carbon-specific ingestion rate (as calculated from the model parameters in Table 2, using Eq. 2) is shown for (supposedly) optimal conditions: corresponding to the maximum growth curve in Figure 2 ($f = 1$). The prediction for furcilia larvae was based on a lower value for the scaled functional response (Table 2).

The data show a lot of scatter, which is inherent to the complications of establishing ingestion rates experimentally. As we express ingestion rates per unit of body weight, errors in the

12

measurement or estimation of the weights may also contribute to the scatter. Furthermore, our prediction assumes a carbon assimilation efficiency of 80%, which may also vary between experiments (a lower efficiency would lead to higher predictions for the ingestion rate, see Table 1). Nevertheless, the predictions are reasonably consistent with the data. The ingestion rates for the furcilia larvae cover a wide range, with values corresponding to the predicted ingestion rates for furcilia and others corresponding better to the predictions for $f = 1$. The ingestion data for furcilia from Ikeda (1984) correspond best to the prediction for this stage, using the lower f as estimated on the growth data from the same experiment (Figure 2). This is thus consistent with our assumption for reduced feeding in this stage. The higher ingestion rates that are found in other studies allow for the possibility that furcilia larvae are capable of growth at the predicted rates for $f = 1$.

For adults, the model parameters suggest that the daily ration should always be less than 5%. However, several authors have reported higher values, as shown in Figure 4. There could be a bias in the experimental method, a lower assimilation efficiency, or these values may represent a short-term peak in ingestion. However, if such high values for the ingestion rate (along with a high assimilation efficiency) would be corroborated, this would require a revision of our parameter set and/or model assumptions (see also Supplement 3).
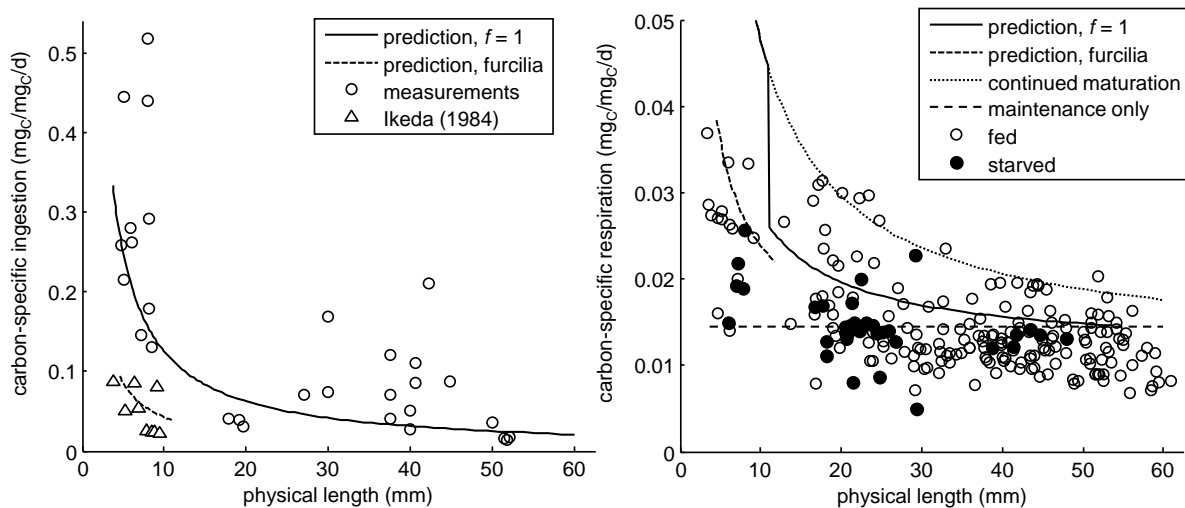

Figure 4. Carbon-specific ingestion rates (left) and respiration rates (right) from the literature, compared to the model predictions using the parameters in Table 2. Separate prediction for furcilia larva, based on the lower predicted ingestion rates (Table 2). For ingestion, only the data from Ikeda (1984) are specifically indicated, derived from the same experiment as the larval growth in Figure 2. For respiration, several predictions are shown (see text), including the minimum estimation based on somatic maintenance costs only. Filled symbols for respiration are studies for individuals incubated for some time at very low food or complete starvation before the measurement.

Respiration rates

The measured respiration rates are compared in Figure 4 to predicted respiration rates using the model parameters in Table 2. It is essential to realise that respiration is a lump sum with contributions from several energy-requiring processes; contributions which depend on the life stage and feeding history of the individuals. Here, we present several predictions: a minimum (maintenance only), a specific estimate for furcilia (low f), and for juveniles/adults a maximum with and without the complete switch from maturation to storage (see Eq. 3, 4). The measured respiration rates should theoretically fall between the highest and lowest lines, as growth and

maturation can likely be decreased or even stopped under starvation. As respiration is measured in the absence of food, the duration of the measurement, as well as the size and condition of the animal, will probably determine whether we observe rates closer to the maximum or to the minimum predictions. The maximum prediction respiration rate (solid line) makes a jump at the start of the juvenile stage, reflecting the switch from maturation to storage (see Eq. 3).

Overall, the observed respiration rates are quite consistent with the predictions. This is even more striking if we consider that the predictions are only based on the growth curves, together with some general conversion factors (Table 2). The data for furcilia are better represented by the specific prediction based on their apparent lower functional response.

Quite a number of data points are below the minimum line, which could point at a conversion problem (e.g., the need for a different respiratory quotient or dry-weight density), or that a lower specific maintenance rate would be more representative for the test conditions. Also, any storage would lead to lower measurements for the carbon-specific respiration rates, as storage is assumed not to require maintenance. Where both starved and fed animals were compared in the same study, the starved animals are lower and closer to the minimum. This indicates the general validity of our interpretation of respiration rates as a lump sum of different physiological processes.

For Figure 4, we did not include respiration data for the non-feeding stages. Detailed data for respiration from the newly-laid egg to calyptopis I are provided in Quetin & Ross (1989), which reveal a linear increase over time, with a sudden increase at hatching (start of nauplius I stage). In contrast, DEBkiss would predict respiration to increase with time squared, which was confirmed for pond snail embryos (Jager et al. 2013). It is unclear what causes this deviation; the metabolic rules for the non-feeding stages of Antarctic krill require further investigation.

Starvation

Data for weight loss on starvation for summer-sampled juveniles/adults were taken from Ikeda & Dixon (1982) and Virtue et al. (1997). The weight decrease was estimated from measurements on the collected moults over time. Body composition did not change much over starvation, and did not suggest a considerable storage compartment in the starting population. Therefore, we assume that these animals burned structure to pay maintenance costs. Data and model prediction (Eq. 5 with parameters from Table 2) are compared in Figure 5 (left panel). Clearly, almost all animals lose less weight than predicted from the specific maintenance rate of Table 2 (prediction 1 in Figure 5). Therefore, it is likely that animals decreased their maintenance costs under these starvation conditions. This is confirmed by the low respiration rate measured at the end of the test in Ikeda & Dixon (1982), which is less than half of the minimum predicted respiration (for maintenance only). Using the measured respiration rate of the starved animals (prediction 2 in Figure 5) to predict weight loss provides a reasonable description for the experiment of Virtue et al. (1997), although the scatter is considerable. The animals in Ikeda & Dixon (1982), however, reveal an even slower decrease in weight (by roughly a factor of two), which is inconsistent with the measured respiration rate in the same experiment. This discrepancy may relate to an error in the measured respiration rate, or in the applied conversions. However, we should also consider that starvation may not have been complete; for example, bacteria might still have provided some level of nutrition for the krill (Virtue et al. 1997).

The right panel of Figure 5 shows the decrease in dry weight upon starvation for furcilia IV, as reported by Meyer & Oettl (2005). These larvae show a more severe rate of weight loss on

starvation than predicted using Eq. 5 (roughly a factor of two). It is thus likely that these larvae are unable to reduce their maintenance costs under food limitation. The measured respiration rates decreased over the first 6 days of starvation (Meyer & Oettl 2005), which likely reflects the cessation of additional energy-requiring processes (growth, maturation). It is these processes that account for the difference between the maximum and minimum predictions for respiration rate in Figure 4. The respiration rate decreased over starvation until it reached a stable minimum of some 2% on carbon basis per day, which is still slightly higher than the predicted minimum in Figure 4, thus supporting the lack of reduction in somatic maintenance on starvation. Some of the costs associated with maturation may not be as easily reduced in larvae, which could explain the higher-than-expected weight loss in the starving larvae (Figure 5). However, the larvae still lose more weight than predicted from the average respiration rate in the same experiment, which implies that they lose more carbon than expected from their use of oxygen.
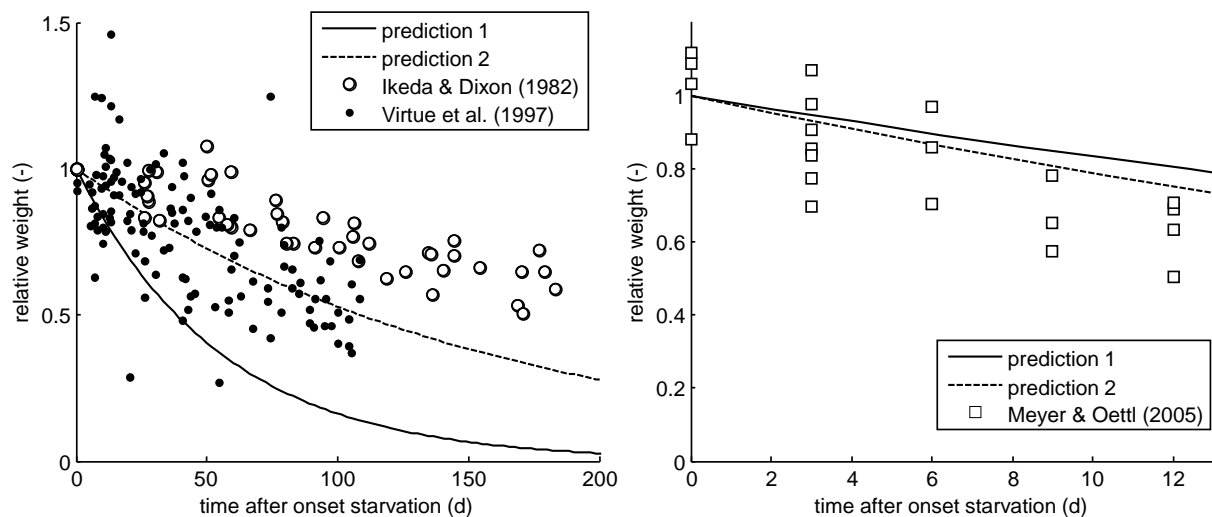

Figure 5. Relative weight loss on starvation. Two model predictions are shown, 1) using the parameters of Table 2 using Eq. 5, and 2) using the observed respiration rate at the end of the test in Ikeda & Dixon (1982), and the average over the test in Meyer & Oettl (2005).

Reproduction

The reproduction rates of Antarctic krill are difficult to estimate; the only estimates are from gravid females that spawned within weeks after collection from the field (and hence with an unknown feeding history). This batch of eggs has been produced from a storage (reproduction buffer) that was built up well before spawning. Using our parameter set, we can predict how long a female should have been eating at maximum rate to be able to produce a batch of a certain size (Eq. 6). This is compared to measured numbers of spawned eggs (see methods section) as a function of body length in Figure 6. The model predicts an increase in batch size with female length (as J_A scales with L^2 in Eq. 6), which is consistent with the observations. According to our parameterised model, a build-up time of 1-5 months is required to cover the observed range in clutch sizes, with most of the data less than 3 months. This does not seem to be very unrealistic, especially as our parameterisation is based on a temperature of 0°C (higher temperatures will shorten these build-up times). Part of the energy required for making a batch of eggs may be formed by the remaining overwintering storage (Virtue et al. 1997, Meyer 2012) at the start of spring. However, even with fully depleted storage, a female may still be able to build up the

material to produce a large batch of eggs in January when feeding conditions are optimal; Ross & Quetin (1986) discuss that positive growth and ovarian development may already start in early spring (September). The large variation in batch size may thus relate to the feeding history of the individual female, and how much of the lipid reserve from the previous summer has been used for overwintering.

The number of spawning events within one season is still under debate (see e.g., Ross & Quetin 1983, Harrington & Ikeda 1986, Nicol et al. 1995). Our current parameterisation allows for one, or perhaps two smaller, clutches of eggs per season, also considering that the females need to build up sufficient storage during late summer and autumn to survive the next winter. A lower value of κ would allow for multiple spawning events, but will also change the predictions for the ingestion and respiration rates (see Supplement 3), as well as the time needed to build up storage for overwintering (see Supplement 2).
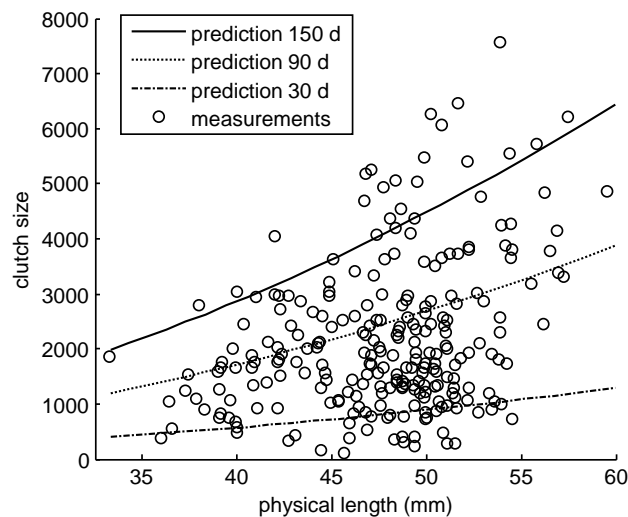

Figure 6. Batch size for reproduction (in numbers of eggs) as function of body size. Model predictions for the potential batch size, given a certain time to build up a reproduction buffer, as provided by Eq. 6.

EVALUATION AND OUTLOOK

DEBkiss offers a simple platform for the explicit and quantitative formalisation of a dynamic energy budget over the entire life cycle. Model parameterisation could be performed using nothing more than growth curves and a few general conversion factors. The small set of model parameters (Table 2) was subsequently able to provide realistic patterns for instantaneous growth, ingestion, respiration, starvation and reproduction, as functions of body size. This efficiency has been achieved by rigorous simplification. Many aspects of krill physiology have been ignored (e.g., changes in composition over ontogeny) or unrecognisably lumped with other processes (e.g., moulting and swimming costs in somatic maintenance). Many of the details on behaviour (e.g., vertical and horizontal migration, seasonal changes in feeding behaviour) and environment (e.g., temperature, ice cover, food availability) are condensed into the scaled functional response (f) and the scaling of rate constants with temperature. Producing realistic life histories thus rests not only on the model parameterisation but also on an accurate representation of the actual value of f and temperature that the individual experiences as a function of time.

16

The main uncertainty in the current parameter set is the value of κ. A value around 0.8 is fairly typical for DEB-based analyses (Kooijman 2013), but in individual cases, values from 0.1 to almost 1 have been established. Selecting a lower value for κ has predictable consequences in our analyses (an alternative analysis using $\kappa = 0.4$ is presented as Supplement 3): to match the observed growth curves, the specific assimilation rate (J_{Am}^{a}) will need to be higher, which implies higher ingestion rates (Figure 4). A lower κ implies a larger maturation flux, which leads to higher maximum respiration rates for furcilia and juveniles (Figure 4). The minimum respiration rate would not be affected as the specific maintenance rate (J_M^{v}) is mainly determined by the curvature of the growth curve. Also, the build-up time for the reproduction buffer (Figure 6) strongly depends on the value of κ, with lower values leading to larger clutch sizes, or shorter build-up times for the storage buffer, thereby allowing multiple spawning events in summer. A crude comparison of model predictions (at two values of κ) and lipid data from field-sampled animals is provided in Supplement 2. However, we currently lack the information to confidently select the most realistic value for κ. Even though we cannot provide a definitive parameterisation for *E. superba*, this analysis clearly shows that physiological traits cannot be viewed in isolation, as they are linked through the rules for the energy budget and constricted by the conservation laws. Therefore, the DEBkiss model is useful to quantitatively test ecophysiological questions regarding overwintering strategies, spawning frequency, minimum food requirements, etc. Finally, this framework can easily be extended to interpret and predict the effects of pollution and other stressors on all of the traits of an individual (Jager & Zimmer 2012), which allows for meaningful extrapolations to the population impacts (Jager et al. 2014).

In principle, the parameter set should remain constant over the entire life cycle, but there are situations in which we are forced to relax this restriction, and allow parameters to change with ontogeny in a structured manner (Kooijman Acc.). Such an adaptation is very likely needed to cover development of the non-feeding stages in *E. superba*, and possibly also to explain the slow growth in furcilia larvae (Figure 2). The slow growth in this stage was also shown in field-sampled animals (Figure 3), and may therefore be an adaptation for dispersal or overwintering, as small individuals require lower food densities to maintain their bodies (Kooijman Acc.). Furthermore, specific attention is needed regarding the overwintering strategy of the juveniles/adults, as there are strong indications they are able to decrease their assimilation and maintenance rates in response to the light regime, irrespective of the available food (Teschke et al. 2007).

In an abstraction of biology, as is the case for the DEB framework, details are inevitably lost by focussing on generality. The model we used is not specific for *E. superba*, and not even specific for aquatic organisms; it is a generic model for invertebrate life cycles. Animals differ in parameter values and hardly in model structure, and parameter values tend to vary in predictable ways (Lika et al. 2011). The DEB framework can be used to compare very different species on a meaningful basis: by comparing model parameters of the energy budget rather than the resulting traits (as in Kooijman 2013). Clearly, more experimental work will be needed to provide the full picture for Antarctic krill, although the present parameterisation already provides a reasonable representation of all traits. This work can thus serve as a starting point for further investigations, and also as a basis for studies on the energetics of other euphausiids. In a broader perspective, DEB models have the potential to provide a common language for researchers working on very different species and/or questions (Alunno-Bruscia et al. 2011), thereby stimulating more diverse research collaborations. Focussing on the similarities between species, rather than their differences, still has a lot to offer for ecology.

LITERATURE CITED

Alunno-Bruscia M, van der Veer HW, Kooijman SALM (2011) The AquaDEB project: physiological flexibility of aquatic animals analysed with a generic dynamic energy budget model (phase II). J Sea Res 66:263-269

Atkinson A, Shreeve RS, Hirst AG, Rothery P, Tarling GA, Pond DW, Korb RE, Murphy EJ, Watkins JL (2006) Natural growth rates in Antarctic krill (*Euphausia superba*): II. Predictive models based on food, temperature, body length, sex, and maturity stage. Limnol Oceanogr 51:973-987

Bengtson Nash SM, Poulsen AH, Kawaguchi S, Vetter W, Schlabach M (2008) Persistent organohalogen contaminant burdens in Antarctic krill (*Euphausia superba*) from the eastern Antarctic sector: a baseline study. Sci Total Environ 407:304-314

Boyd CM, Heyraud M, Boyd CN (1984) Feeding of the Antarctic krill *Euphausia superba*. J Crustac Biol 4:123-141

Clarke A, Quetin LB, Ross RM (1988) Laboratory and field estimates of the rate of fecal pellet production by Antarctic krill, *Euphausia superba*. Mar Biol 98:557-563

Daly KL (1990) Overwintering development, growth, and feeding of larval *Euphausia superba* in the Antarctic marginal ice zone. Limnol Oceanogr 35:1564-1576

Daly KL (1998) Physioecology of juvenile Antarctic krill (*Euphausia superba*) during spring in ice-covered seas. In: Lizotte MP, Arrigo KR (eds) Antarctic sea ice: biological processes, interactions and variability. American Geophysical Union, Washington, D.C., US

Daly KL (2004) Overwintering growth and development of larval *Euphausia superba*: an interannual comparison under varying environmental conditions west of the Antarctic Peninsula. Deep-Sea Research Part II 51:2139-2168

Denys CJ, McWhinnie MA (1982) Fecundity and ovarian cycles of the Antarctic krill *Euphausia superba* (Crustacea, Euphausiacea). Can J Zoolog 60:2414-2423

Haberman KL, Quetin LB, Ross RM (2003) Diet of the Antarctic krill (*Euphausia superba* Dana): I. Comparisons of grazing on *Phaeocystis antarctica* (Karsten) and *Thalassiosira antarctica* (Comber). J Exp Mar Biol Ecol 283:79-95

Hagen W, Kattner G, Terbrüggen A, Van Vleet ES (2001) Lipid metabolism of the Antarctic krill *Euphausia superba* and its ecological implications. Mar Biol 139:95-104

Harrington SA, Ikeda T (1986) Laboratory observations on spawning, brood size and egg hatchability of the Antarctic krill *Euphausia superba* from Prydz Bay, Antarctica. Mar Biol 92:231-235

Hirche HJ (1983) Excretion and respiration of the Antarctic krill *Euphausia superba*. Polar Biol 1:205-209

Hofmann EE, Lascara CM (2000) Modeling the growth dynamics of Antarctic krill *Euphausia superba*. Mar Ecol Prog Ser 194:219-231

Huntley M, Brinton E (1991) Mesoscale variation in growth and early development of *Euphausia superba* Dana in the western Bransfield Strait region. Deep-Sea Res 38:1213-1240

Ikeda T (1981) Metabolic activity of larval stages of Antarctic krill. Antarctic Journal of the US 16:161-162

Ikeda T (1984) Development of the larvae of the Antarctic krill (*Euphausia superba* Dana) observed in the laboratory. J Exp Mar Biol Ecol 75:107-117

Ikeda T (1985a) Life history of Antarctic krill *Euphausia superba*: a new look from an experimental approach. Bull Mar Sci 37:599-608

Ikeda T (1985b) Metabolic rate and elemental composition (C and N) of embryos and non-feeding early larval stages of Antarctic krill (*Euphausia superba* Dana). J Exp Mar Biol Ecol 90:119-127

Ikeda T (1987) Mature Antarctic krill (*Euphausia superba* Dana) grown from eggs in the laboratory. J Plankton Res 9:565-569

Ikeda T, Dixon P (1982) Body shrinkage as a possible over-wintering mechanism of the Antarctic krill, *Euphausia superba* Dana. J Exp Mar Biol Ecol 62:143-151

Ikeda T, Mitchell AW (1982) Oxygen uptake, ammonia excretion and phosphate excretion by krill and other Antarctic zooplankton in relation to their body size and chemical composition. Mar Biol 71:283-298

Ishii H, Omori M, Maeda M, Watanabe Y (1987) Metabolic rates and elemental composition of the Antarctic krill, *Euphausia superba* Dana. Polar Biol 7:379-382

Jager T, Barsi A, Hamda NT, Martin BT, Zimmer EI, Ducrot V (2014) Dynamic energy budgets in population ecotoxicology: applications and outlook. Ecol Modell 280:140-147

Jager T, Martin BT, Zimmer EI (2013) DEBkiss or the quest for the simplest generic model of animal life history. J Theor Biol 328:9-18

Jager T, Zimmer EI (2012) Simplified Dynamic Energy Budget model for analysing ecotoxicity data. Ecol Modell 225:74-81

Kato M, Segawa S, Tanoue E, Murano M (1982) Filtering and ingestion rates of the Antarctic krill, *Euphausia superba* Dana. Trans Tokyo Univ Fish 5:167-175

Kawaguchi S, Candy SG, King R, Naganobu M, Nicol S (2006) Modelling growth of Antarctic krill. I. Growth trends with sex, length, season, and region. Mar Ecol Prog Ser 306:1-15

Kooijman SALM (2001) Quantitative aspects of metabolic organization: a discussion of concepts. Phil Trans R Soc B 356:331-349

Kooijman SALM (2013) Waste to hurry: dynamic energy budgets explain the need of wasting to fully exploit blooming resources. Oikos 122:348-357

Kooijman SALM (Acc.) Metabolic acceleration in animal ontogeny: an evolutionary perspective. J Sea Res In press. DOI 10.1016/j.seares.2014.06.005

Lika K, Kearney MR, Freitas V, Van der Veer HW, Van der Meer J, Wijsman JWM, Pecquerie L, Kooijman SALM (2011) The "covariation method" for estimating the parameters of the standard Dynamic Energy Budget model I: Philosophy and approach. J Sea Res 66:270-277

Meyer B (2012) The overwintering of Antarctic krill, *Euphausia superba*, from an ecophysiological perspective. Polar Biol 35:15-37

Meyer B, Atkinson A, Blume B, Bathmann UV (2003) Feeding and energy budgets of larval Antarctic krill *Euphausia superba* in summer. Mar Ecol Prog Ser 257:167-177

Meyer B, Atkinson A, Stübing D, Oettl B, Hagen W, Bathmann UV (2002) Feeding and energy budgets of Antarctic krill *Euphausia superba* at the onset of winter I. Furcilia III larvae. Limnol Oceanogr 47:943-952

Meyer B, Auerswald L, Siegel V, Spahić S, Pape C, Fach BA, Teschke M, Lopata AL, Fuentes V (2010) Seasonal variation in body composition, metabolic activity, feeding, and growth of adult krill *Euphausia superba* in the Lazarev Sea. Mar Ecol Prog Ser 398:1-18

Meyer B, Fuentes V, Guerra C, Schmidt K, Atkinson A, Spahic S, Cisewski B, Freier U, Olariaga A, Bathmann U (2009) Physiology, growth, and development of larval krill *Euphausia superba* in autumn and winter in the Lazarev Sea, Antarctica. Limnol Oceanogr 54:1595-1614

Meyer B, Oettl B (2005) Effects of short-term starvation on composition and metabolism of larval Antarctic krill *Euphausia superba*. Mar Ecol Prog Ser 292:263-270

Nicol S, De la Mare WK, Stolp M (1995) The energetic cost of egg production in Antarctic krill (*Euphausia superba* Dana). Antarct Sci 7:25-30

Nicol S, Foster J, Kawaguchi S (2012) The fishery for Antarctic krill - recent developments. Fish Fish 13:30-40

Nisbet RM, Muller EB, Lika K, Kooijman SALM (2000) From molecules to ecosystems through dynamic energy budget models. J Anim Ecol 69:913-926

Pakhomov EA, Atkinson A, Meyer B, Oettl B, Bathmann U (2004) Daily rations and growth of larval krill *Euphausia superba* in the Eastern Bellingshausen Sea during austral autumn. Deep-Sea Res 51:2185-2198

Pakhomov EA, Perissinotto R, Froneman PW, Miller DGM (1997) Energetics and feeding dynamics of *Euphausia superba* in the South Georgia region during the summer of 1994. J Plankton Res 19:399-423

Pecquerie L, Fablet R, de Pontual H, Bonhommeau S, Alunno-Bruscia M, Petitgas P, Kooijman SALM (2012) Reconstructing individual food and growth histories from biogenic carbonates. Mar Ecol Prog Ser 447:151-164

Quetin LB, Ross RM (1989) Effects of oxygen, temperature and age on the metabolic-rate of the embryos and early larval stages of the Antarctic krill *Euphausia superba* Dana. J Exp Mar Biol Ecol 125:43-62

Quetin LB, Ross RM, Frazer TK, Amsler MO, Wyatt-Evens C, Oakes SA (2003) Growth of larval krill, *Euphausia superba*, in fall and winter west of the Antarctic Peninsula. Mar Biol 143:833-843

Ross RM, Quetin LB (1983) Spawning frequency and fecundity of the Antarctic krill *Euphausia superba*. Mar Biol 77:201-205

Ross RM, Quetin LB (1986) How productive are Antarctic krill. Bioscience 36:264-269

Ross RM, Quetin LB (1989) Energetic cost to develop to the first feeding stage of *Euphausia superba* Dana and the effect of delays in food availability. J Exp Mar Biol Ecol 133:103-127

Ross RM, Quetin LB, Baker KS, Vernet M, Smith RC (2000) Growth limitation in young *Euphausia superba* under field conditions. Limnol Oceanogr 45:31-43

Saraiva S, van der Meer J, Kooijman SALM, Witbaard R, Philippart CJM, Hippler D, Parker R (2012) Validation of a Dynamic Energy Budget (DEB) model for the blue mussel *Mytilus edulis*. Mar Ecol Prog Ser 463:141-158

Schnack SB (1985) Feeding by *Euphausia superba* and copepod species in response to varying concentrations of phytoplankton. In: Siegfried WR, Condy PR, Laws RM (eds) Antarctic Nutrient Cycles and Food Webs. Springer, Berlin, Germany

Segawa S, Kato M, Murano M (1982) Respiration and ammonia excretion rates of the Antarctic krill, *Euphausia superba* Dana. Trans Tokyo Univ Fish 5:177-187

Sousa T, Domingos T, Poggiale JC, Kooijman SALM (2010) Dynamic energy budget theory restores coherence in biology. Phil Trans R Soc B 365:3413-3428

Teschke M, Kawaguchi S, Meyer B (2007) Simulated light regimes affect feeding and metabolism of Antarctic krill, *Euphausia superba*. Limnol Oceanogr 52:1046-1054

Teschke M, Kawaguchi S, Meyer B (2008) Effects of simulated light regimes on maturity and body composition of Antarctic krill, *Euphausia superba*. Mar Biol 154:315-324

Torres JJ, Aarset AV, Donnelly J, Hopkins TL, Lancraft TM, Ainley DG (1994) Metabolism of Antarctic micronektonic Crustacea as a function of depth of occurrence and season. Mar Ecol Prog Ser 113:207-219

Virtue P, Nichols PD, Nicol S (1997) Dietary-related mechanisms of survival in *Euphausia superba*: biochemical changes during long-term starvation and bacteria as a possible source of nutrition. In: Battaglia B, Valencia J, Dalton DWH (eds) Antarctic communities: species, structure and survival. Cambridge University Press, Cambridge, UK